ACS NANO

Cite This: *ACS Nano* XXXX, XXX, XXX−XXX

www.acsnano.org

ARTICLE

Light-Induced Reversible DNA Ligation of Gold Nanoparticle Superlattices

Angela F. De Fazio,[†] Afaf H. El-Sagheer,[‡,§] Jason S. Kahn,[∥,⊥] Iris Nandhakumar,[#] Matthew Richard Burton,[□] Tom Brown,[‡] Otto L. Muskens,[†,○] Oleg Gang,*[,∥,⊥,¶] and Antonios G. Kanaras*[,†,○]

[†]School of Physics and Astronomy, Faculty of Engineering and Physical Sciences, University of Southampton, Southampton, SO17 1BJ, U.K.

[‡]Chemistry Research Laboratory, Department of Chemistry, University of Oxford, 12 Mansfield Road, Oxford, OX1 3TA, U.K.

[§]Chemistry Branch, Department of Science and Mathematics, Faculty of Petroleum and Mining Engineering, Suez University, Suez 43721, Egypt

[∥]Center for Functional Nanomaterials, Brookhaven National Laboratory, Upton, New York 11973, United States

[⊥]Department of Chemical Engineering, Columbia University, New York, New York 10027, United States

[#]School of Chemistry, Faculty of Engineering and Physical Sciences, University of Southampton, Southampton, SO17 1BJ, U.K.

[□]SPECIFIC-IKC, Materials Research Centre, College of Engineering, Swansea University, Bay Campus, Fabian Way, Swansea, SA1 8EN, U.K.

[¶]Department of Applied Physics and Applied Mathematics, Columbia University, New York, New York 10027, United States

[○]Institute for Life Sciences, University of Southampton, Southampton, SO17 1BJ, U.K.

Supporting Information

ABSTRACT: **DNA-mediated self-assembly of nanoparticles has been of great interest because it enables access to nanoparticle superstructures that cannot be synthesized otherwise. However, the programmability of higher order nanoparticle structures can be easily lost under DNA denaturing conditions. Here, we demonstrate that light can be employed as an external stimulus to master the stability of nanoparticle superlattices (SLs) *via* the promotion of a reversible photoligation of DNA in SLs. The oligonucleotides attached to the nanoparticles are encoded to ligate using 365 nm light, effectively locking the SLs and rendering them stable under DNA denaturing conditions. The reversible process of unlocking these structures is possible by irradiation with light at 315 nm, recovering the structures to their natural state. Our work inspires an alternative research direction toward postassembly manipulation of nanoparticle superstructures using external stimuli as a tool to enrich the library of additional material forms and their application in different media and environments.**

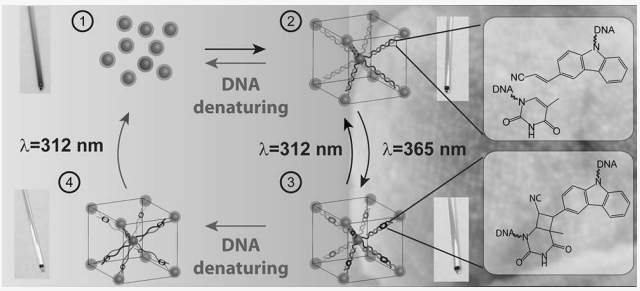

KEYWORDS: *DNA, nanoparticles, photochemical ligation, self-assembly, superlattices*

Bottom-up approaches for the 3D organization of nanoparticles into larger structures are of utmost importance for the fabrication of materials with improved properties.[1] Such approaches can provide cost-effective and broader access to structures that are currently at the limit of our lithographic capabilities and could enable greater control over the fabrication of programmable and reconfigurable metamaterials.

Several methods for the organization of nanoparticles into larger structures have been reported, involving different types of weak nanoparticle interactions or application of external fields.[2−6] For example, in 1995 the Pileni[7] and Bawendi[8] groups reported the discovery of electrostatically directed superlattice assemblies of Ag_2S and CdSe, respectively. Two- and three-dimensional superlattices were also obtained *via* molecular interactions,[9] for instance between alkylthiol-functionalized gold nanoparticles, as reported by Brust *et al.*[10] and Landman and co-workers.[11] Polymers and block copolymers have also been extensively used to direct the ordered assembly of nanoparticles,[12−16] while in other cases

Received: February 15, 2019
Accepted: April 1, 2019

DOI: 10.1021/acsnano.9b01294
ACS Nano XXXX, XXX, XXX−XXX

Scheme 1. Reversible photochemical ligation of nanoparticle superlattices. Nanoparticles conjugated with oligonucleotides are hybridized under the appropriate conditions to form superlattices. One batch of oligonucleotide-coated nanoparticles contains a 3-cyanovinylcarbazole modification, which can react upon irradiation at λ = 365 nm with an adjacent thymine in the complementary strand, to form an interstrand chemical bond. This photochemical process can be reversed upon irradiation with light at λ = 312 nm.

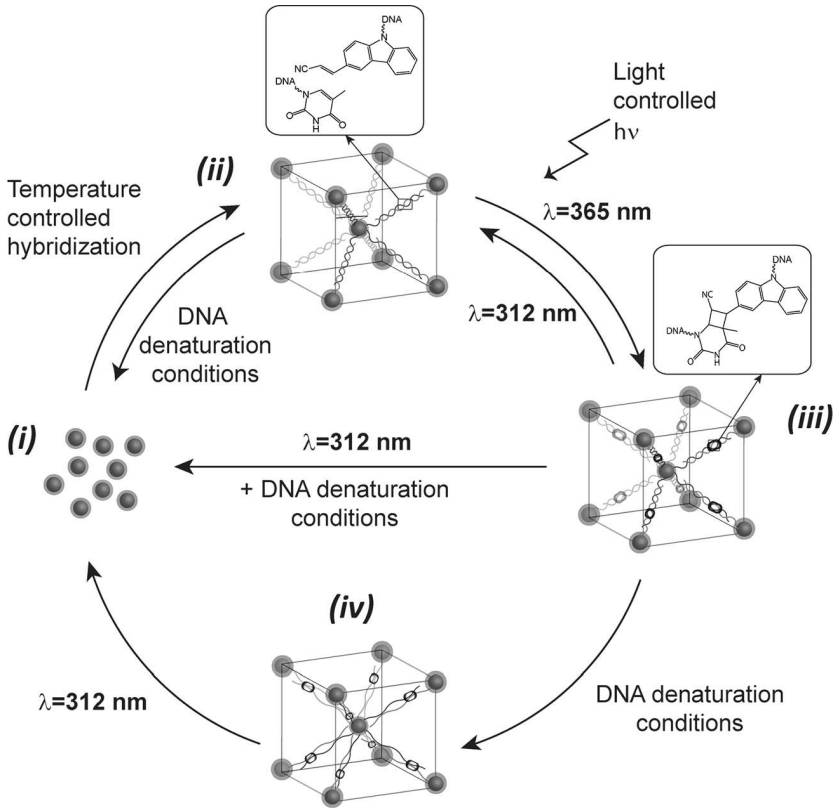

proteins,[17,18] peptides,[19,20] and enzymes[21,22] have been employed to organize nanostructures.

Among all these strategies, the use of oligonucleotides to assemble nanoparticles has been demonstrated to be powerful and versatile. Oligonucleotides possess high selectivity and specificity for complementary sequences, versatility in the structures that can be constructed, and the ability to be modified chemically with a variety of functional groups. The groups of Mirkin[23] and Alivisatos[24] were the first to report the functionalization of gold nanoparticles with oligonucleotides in 1996. Further exploitation of oligonucleotide-coated nanoparticles allowed the formation of programmed nanoparticle assemblies, starting from nanoparticle dimers and trimers to larger structures. However, it was not until 2008 that SLs of oligonucleotide-coated gold nanoparticles were reported independently by the groups of Mirkin[25] and Gang.[26] In those works, both groups described the experimental conditions and oligonucleotide design rules to form body-centered cubic and face-centered cubic organized gold nanoparticle assemblies.

Since then, a variety of SLs have been fabricated[26−29] using nanoparticles of different chemical compositions, such as silver[30] and cadmium selenide,[31] and different shapes, including cubes or octahedra, to guide binding interactions based on the topology of the particles.[32] Specifically engineered oligonucleotides were also utilized to arrange NPs in previously unattainable particle arrangements not directly achievable through traditional means, such as the use of DNA origami frames to systematically collocate particles in a diamond lattice.[33] Another example was a convertible lattice obtained by means of reconfigurable DNA strands, which were able to switch between two states that yield two different lattice structures.[34]

Although a large variety of SLs have been reported, efforts have mostly focused on tuning the size, shape, and composition of nanoparticles as well as simple oligonucleotide characteristics such as the length and the number of complementary base pairs. A common limitation of SLs reported to date is their inherent instability under DNA-denaturing conditions due to dehybridization of double-stranded DNA (dsDNA) into the component single strands (ssDNA). DNA−gold nanoparticle superlattices are readily disassembled in conditions that do not favor DNA hybridization such as elevated temperatures, low ionic strengths, and other harsh environments such as low or high pH.

Attempts to tackle this issue have focused mainly on the intercalation of molecules[35] or ions[36] within the DNA duplex. Alternatively, one could envisage methods to ligate the oligonucleotides within nanoparticle assemblies. Indeed, such methods have already been developed for nanoparticle oligomers and for amorphous DNA−nanoparticle aggregations. In 2003, the Brust group reported the use of ligase enzymes as biomolecular tools for the covalent linking of DNA−gold nanoparticle amorphous aggregates,[37] while in 2008 the Alivisatos group[22] reported the scaled-up production of covalently bound DNA gold nanoparticle dimers, also using

DOI: 10.1021/acsnano.9b01294
ACS Nano XXXX, XXX, XXX−XXX

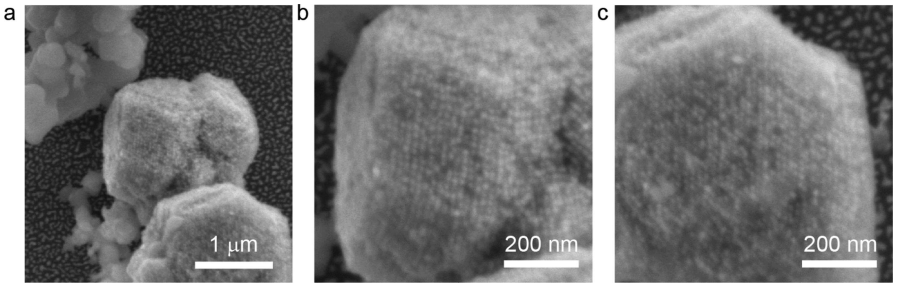

Figure 1. Scanning electron micrographs of gold nanoparticle–DNA superlattices (a) and higher-magnification images where the organization of gold nanoparticles can be observed (b, c).

DNA ligases. Recently, our group has developed two separate methods to chemically and photochemically ligate DNA-coated gold nanoparticles in dimer, trimer, and tetramer structures. In the first method, DNA–gold nanoparticles were spontaneously ligated to dimers and trimers using oligonucleotides functionalized with an azide and a strained cyclooctyne group, respectively.[38] In the second method,[39] DNA–gold nanoparticles were ligated to dimer, trimer, and tetramer structures employing a photoreactive chemical group (3-cyanovinylcarbazole) within the DNA sequence, which upon irradiation with λ = 365 nm light cross-linked the DNA strands. Subsequent, irradiation of the cross-linked DNA with λ = 312 nm light resulted in de-cross-linking of the DNA strands, and this reaction was reversible.

Here we demonstrate the use of 3-cyanovinylcarbazole as a photochemical tool to reversibly ligate gold nanoparticle SLs using light. By employing this tool, we are able to successfully fabricate light-responsive materials with enhanced stability without losing the advantage of the reversible hybridization and programmable functionalities typical of complementary oligonucleotides. Tolerance against DNA denaturing conditions demonstrates the robust character and stability of the superlattices, providing an advanced programmable element and design tool that could potentially be exploited for a variety of applications, including on-demand destruction, local patterning, and even structuring within the scale of single SLs.

RESULTS AND DISCUSSION

Scheme 1 shows the principle of our methodology, which is the ligation of the DNA in the formed nanoparticle SLs and the distinct role of this covalent cross-linking as a tool in combination with the thermal induction of nanoparticle crystal formation. The chemical modification introduced within one set of the ssDNA strands is a cyanovinylcarbazole, which is able to form a covalent bond with an adjacent activated double bond upon irradiation with UV light. Stages (i) and (ii) represent the conventional phases of the reversible SLs' formation using thermal control of DNA hybridization through a thermal annealing procedure. Stage (iii) is reached through the exposure of the SLs to UV light at λ = 365 nm, causing the formation of a cyclobutane between the cyanovinyl moiety on the carbazole on one ssDNA of a dsDNA duplex and the 5,6-double bond on the thymine base on the secondary ssDNA of the duplex *via* a [2+2] photocycloaddition.[40,41] In our work, the SLs were irradiated for 30 min at λ = 365 nm to induce cross-linking between two hybridized DNA strands. Reversibility of the ligation step (ii)–(iii) is achieved by illuminating the cross-linked DNA–AuNPs (phase (iii)) with light at λ = 312 nm to yield the nonligated oligonucleotides. Under DNA denaturing conditions, the ligation between the DNA strands prevents a collapse of the crystal structure of the SLs, resulting in maintenance of the BCC crystal (phase (iv)) with dehybridized DNA strands.

Formation of DNA–Nanoparticle Superlattices. Following previously established protocols,[42] we produced high-quality SLs consisting of gold nanoparticles functionalized with complementary DNA strands utilizing oligonucleotides that do not contain any chemical modification (see Table S1 and Figure S2 for the relevant DNA sequences and nanoparticle size distribution). Briefly, two batches of 14 nm AuNPs were functionalized[43] with a dense shell of complementary thiol-modified single-stranded DNA. The resulting DNA–AuNPs were mixed in equimolar amounts in buffer (10 mM phosphate buffer with 0.3 M NaCl) and were transferred to a ThermoCycler. Heating above the DNA melting temperature and a controlled cooling/annealing (0.1 °C/10 min) yielded SLs with a body-centered-cubic crystal structure. Figure 1 shows scanning electron microscopy (SEM) images for a body-centered-cubic SL sample. In (a), a lower-magnification image shows the sharp facets of the crystals, while in (b) and (c) corresponding zoomed-in pictures display ordered arrangements of the individual nanoparticles (the corresponding small-angle X-ray scattering pattern and a higher magnification SEM image of the nanoparticles' organization are shown in Figure S3).

Stability of DNA–Nanoparticle Superlattices under DNA Denaturing Conditions. The same experimental protocol as above was followed to form SLs employing gold nanoparticles functionalized with cyanovinylcarbazole-modified DNA strands (Figure S1). Figure 2 shows a comparison between NPs assembled using nonmodified and cyanovinylcarbazole-modified oligonucleotides, with corresponding schemes of the nanoparticle assemblies. After the crystallization procedure, both sets of strands yielded a black aggregate that sediments at the bottom of the capillary (Figure 2a and b). Upon irradiation with light at λ = 365 nm and subsequent transfer to DNA denaturing conditions, the aggregated state is retained only for the assemblies composed of the modified DNA strands (the black pellet is still observed at the bottom of the capillary, Figure 2c), while the particles previously held together by the set of conventional strands are released in suspension, as observed by the absence of the pellet at the bottom and the red color of the suspension, a typical property of 14 nm colloidal gold nanoparticles (Figure 2d).

Small-angle X-ray scattering (SAXS) was employed to study the crystal structure of the nanoparticle assemblies in more detail. Figure 3 shows the SAXS patterns for the SLs made with the cyanovinylcarbazole-modified DNA strands (ii, black line).

DOI: 10.1021/acsnano.9b01294
ACS Nano XXXX, XXX, XXX–XXX

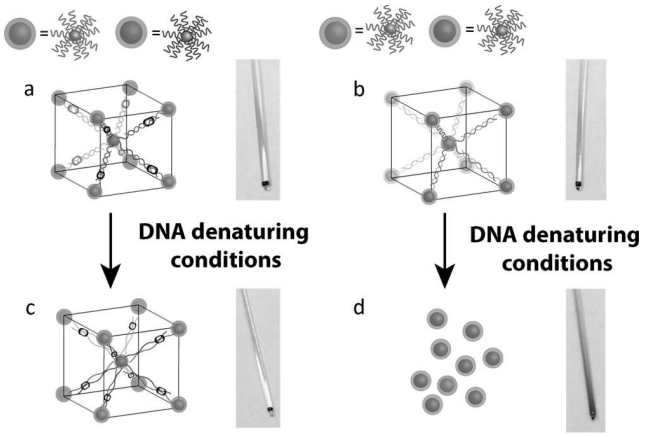

Figure 2. Schematic illustration showing lattices produced from a set of oligonucleotides with cyanovinylcarbazole-modified strands (a), following light illumination at λ = 365, and without modification (b). Optical images of capillaries containing superlattices in native (a and b at the top) and denaturing (c and d at the bottom) conditions are also shown. While the crystals assembled with the carbazole-containing strands remain aggregated upon denaturation (c), the superlattices assembled with the conventional oligonucleotides yielded free NPs upon denaturation, as evidenced by the color change observed in the unmodified sample (d).

From the relative intensity and the position of the peaks it is possible to assign the pattern to a body-centered cubic configuration, where the lattice parameter a was calculated from the relation with the interplane distance d_{hkl} as $a = d_{hkl}\sqrt{h^2 + k^2 + l^2}$ In turn, d_{hkl} was calculated from Bragg's law as $d_{hkl} = 2\pi/q_{hkl}$. The nearest neighbor distance, core-to-core, could be calculated from the cubic geometry of the configuration, and it was found to be 27 nm, in agreement with the predicted value (28 nm) based on the NP diameters and the DNA length. An average crystallite size of ~0.4 μm was estimated from the scattering correlation length $\xi \approx 2\pi/\Delta q$.[44] Further SAXS measurements were carried out to test the effectiveness of the cyanovinylcarbazole-modified DNA nanoparticles in retaining their crystal structure. The scattering patterns of the superlattices after irradiation at λ = 365 nm and subsequent denaturation are shown by the curves labeled (iii, gray) and (iv, red). A marked difference was observed in the SAXS spectrum for SLs when applying denaturing conditions. In the case of the light-active SLs, after irradiation with light at λ = 365 nm and subsequent denaturation, the pattern shows the same number and intensity ratio of the peaks, demonstrating the integrity of the crystal structure. Interestingly, a noticeable shift of the peaks toward lower q-values was observed, which implies a wider distance between NPs in the lattice. We found that the nearest neighbor distance was shifted from 27 nm (in native conditions) to 31 nm for SLs in denaturing conditions. This observation is consistent with an interpretation of DNA dehybridization induced by the denaturing conditions, which relaxes the oligonucleotide strands while the NPs are still held together by the cross-linking between the oligonucleotide strands. As a control, the SAXS profile for irradiated and denatured crystals formed by unmodified DNA strands is also reported in Figure S4, showing no signs of ordered structures, confirming that in the absence of the carbazole modification, irradiating with 365 nm light does not induce DNA cross-linking itself, and thus all crystalline ordering is lost upon DNA dehybridization.

To test the reversibility of the process, DNA-cross-linked superlattices were irradiated with 312 nm light for 30 min and

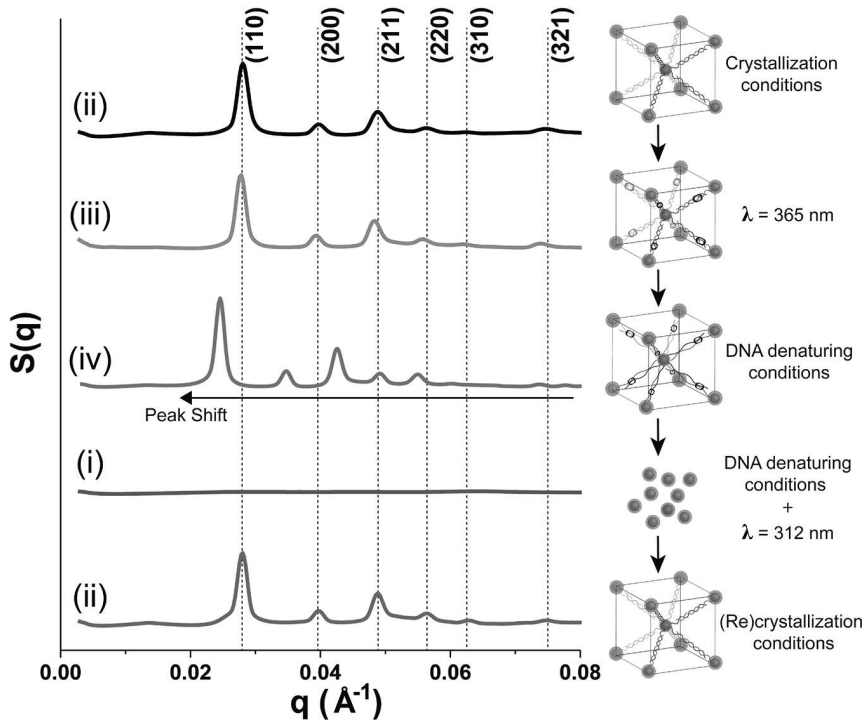

Figure 3. SAXS measurements for nanoparticle superlattices (ii, black), DNA-cross-linked nanoparticle superlattices (iii, gray), DNA-cross-linked nanoparticle superlattices under DNA denaturing conditions (iv, red), DNA-de-cross-linked nanoparticle superlattices under DNA denaturing conditions (i, blue), and recrystallized nanoparticle superlattices (ii, green).

DOI: 10.1021/acsnano.9b01294
ACS Nano XXXX, XXX, XXX−XXX

then subjected to DNA denaturing conditions. During this procedure, a color change in the solution was observed indicating DNA dehybridization and therefore disassembly of the superlattices. As shown in Figure 3, the relevant SAXS pattern (blue line) of the laser-irradiated SLs under DNA denaturing conditions did not show any peaks, which also confirmed the disassembly of the nanoparticles. Furthermore, the disassembled particles were optically characterized and their spectrum was compared to that of the AuNPs coated with oligonucleotides, recorded prior to the initial step of crystallization. As shown in Figure S5, the two spectra are superimposable, with no peak shift or broadening observed for the DNA-coated nanoparticles after UV light exposure, indicating that the short-term UV radiation did not affect the colloidal dispersibility of the nanoparticles.

The function of the oligonucleotides on the surface of the nanoparticles was confirmed by an additional crystallization step. The disassembled nanoparticles were purified and concentrated via centrifugation, redispersed in DNA hybridization buffer (0.01 M phosphate buffer, 0.3 M NaCl), and subjected to another thermocycle. The bottom curve (ii, green) in Figure 3 depicts the SAXS analysis of the recrystallized sample. The positions and relative intensity of the peaks are comparable to the corresponding ones for the pristine crystals, thus demonstrating the robust nature of the DNA strands on the nanoparticles after subsequent steps of heating/cooling and UV light irradiation.

To demonstrate the universal nature of our method, we performed a similar study using silver nanoparticles (AgNPs). AgNPs with a size of 15 ± 6 nm were synthesized by slight modifications to previously reported protocols (Figure S6).[43,45] These particles were coated with a dense shell of oligonucleotides (Table S1) and used in further experiments. Figure S7 shows SEM images obtained from AgNP superlattices (AgNP SLs). The SLs in these images have dimensions of about 1 μm in size with sharp edges and well-defined facets. Figure S8 shows quartz capillaries containing AgNP SLs assembled with conventional (right) or carbazole-modified (left) oligonucleotides after irradiation at λ = 365 nm, with corresponding schemes of the structure. After transfer to DNA denaturing conditions, the SLs without the carbazole modification do not retain the aggregated state, yielding a yellow-colored suspension of free AgNPs in solution. SAXS data are shown in Figure S9. Similar peak patterns to that for the gold SLs were obtained for the native SLs (Figure S9 (i)), the DNA-cross-linked SLs (ii), and the DNA-cross-linked and DNA-denatured SLs. In the latter, a slight shift toward lower q-values was observed, indicating a relaxation of the lattice due to DNA dehybridization. A similar observation was also found for AuNP SLs. Likewise, AgNP SLs irradiated at λ = 312 nm and transferred to DNA denaturing conditions did not show any peaks in SAXS, as expected for colloidal disassembled particles. The disassembled nanoparticles were also optically characterized (Figure S10) and compared to the pristine particles prior to assembly, confirming that neither the AgNPs nor the surface DNA strands were affected by the crystallization and irradiation procedure.

CONCLUSION

In conclusion, we have successfully developed a light-responsive approach to manipulate DNA–nanoparticle SLs. This approach enables the reversible DNA ligation of gold nanoparticle SLs, which retain their 3D structure in DNA denaturing conditions. The universal character of this method was demonstrated by the formation of DNA-ligated silver nanoparticle SLs. Future work could explore the transfer of cross-linked SLs to different liquid or solid-state environments, lifting some of the restrictions of conventional DNA-based technologies. In addition to improving the robustness of the crystal as a whole, one can envisage alternative synthesis strategies involving partial incorporation of ligating groups into the crystal, for example to achieve hollow structures or even in the 3D printing of nanocrystals using direct laser writing.

EXPERIMENTAL METHODS

Commercially available reagents and solvents were purchased from Sigma-Aldrich and used without further purification. Standard DNA phosphoramidites, solid supports (controlled pore glass, CPG), and additional reagents were purchased from Link Technologies, Glen Research, and Applied Biosystems. NAP Sephadex gel filtration columns were purchased from GE Healthcare and used according to the manufacturer's instructions. Oligonucleotides were synthesized on an Applied Biosystems 394 automated DNA/RNA synthesizer using a standard 1.0 μmol phosphoramidite cycle of acid-catalyzed detritylation, coupling, capping, and iodine oxidation. Stepwise coupling efficiencies and overall yields were >98.0% as determined by the automated trityl cation conductivity monitoring facility. 3′-Thiol-modifier C6 S-S solid support (catalogue no: 20-2938) and 3-cyanovinylcarbazole phosphoramidite (catalogue no: 10-4960) were purchased from Glen Research. Assembly of the DNA-NPs was performed in an Applied BioSystems ProFlex PCR thermal cycler. Transmission electron microscopy (TEM) images were obtained on a Hitachi H7000 transmission electron microscope operating at a bias voltage of 75 kV. SEM images were obtained on a Jeol JSM 7500F field-emission gun SEM, with a resolution of 1 nm at 15 kV, operating between 0.5 and 30 kV. UV–visible spectra were acquired using a UV–1601 Shimadzu UV–visible spectrophotometer over the range 200 to 800 nm. SAXS measurements were performed at the Complex Materials Scattering (CMS) beamline of the National Synchrotron Light Source II (NSLS-II, Brookhaven National Lab, Upton, USA). The scattering data were collected with a MAR CCD area detector and converted to 1D scattering intensity *vs* wave vector transfer, $q = (4\pi/\lambda)\sin(\theta/2)$, where λ = 0.8551 Å and θ are the wavelength of incident X-ray and the scattering angle, respectively. The scattering angle was calibrated using silver behenate as a standard. The structure factor $S(q)$ was calculated as the ratio between the background-corrected 1D scattering intensities extracted by angular averaging of CCD images for assembled systems and dissociated particles.

Synthesis of Gold Nanoparticles. The synthesis of 14 ± 1 nm gold nanoparticles was carried out following previously reported protocols.[46,47] A sodium tetrachloroaurate solution (1 mL, 100 mM) was brought to boil while stirring. To this was added a sodium citrate solution (5 mL, 2 wt %), and the solution was stirred for a further 15 min. Then, the reaction mixture was left to cool while stirring. Particles were purified by filtering the solution through a 0.45 Millipore filter and were redispersed in 10 mL of Milli-Q water.

Synthesis of Silver Nanoparticles. The synthesis of 15 ± 6 nm AgNPs was performed with slight modifications of previously reported protocols.[45] Sodium citrate (1 mL, 5 mM) and tannic acid (1 mL, 0.025 mM) were added to a flask containing 98 mL of Milli-Q water. This solution was heated under vigorous stirring until boiling. $AgNO_3$ (1 mL, 25 mM) was injected into the boiling solution, which became bright yellow. After 15 min, particles of ∼15 nm in size were obtained. Purification was performed by centrifugation (10 000 rpm, 20 min, 3×) and the collected NPs were dispersed in 10 mL of Milli-Q water.

Oligonucleotide Functionalization and Assembly of NPs. In a typical experiment, citrate-coated NPs (10 pmol, 500 μL) were incubated overnight with thiol-modified oligonucleotides (800 pmol, 40 μL), and phosphate buffer (60 μL, 0.1 M) was added to achieve a final concentration of 0.01 M. Six additions of a NaCl solution (106 μL, 2 M) over a period of 8 h were introduced to achieve a final salt

DOI: 10.1021/acsnano.9b01294
ACS Nano XXXX, XXX, XXX–XXX

concentration of 0.3 M. The resulting ssDNA-coated AuNPs were then purified by three subsequent centrifugation steps (16 400 rpm, 10 min). Finally, the conjugates were stored in Milli-Q water at 4 °C. Two batches of NPs (10 pmol, 1 mL) decorated with complementary DNA strands were incubated in hybridization buffer (10 mM phosphate buffer, 0.3 M NaCl) at 70 °C (above the melting temperature of the DNA duplex) and slowly cooled to 25 °C using a programmable thermal cycler (rate 0.1 °C/10 min). Nanoparticle assemblies were sedimented at the bottom of the tube, and the supernatant was clear.

Light-Induced Reversible DNA Cross-Linking between Nanoparticles. DNA cross-linking was performed by transferring 200 μL of DNA-NP crystals on a plate in an ice-bath and placed under UV-A light (centered at λ = 365 nm, 50 mW/cm^2, 30 min, at a distance of 4 cm from the UV lamp). DNA de-cross-linking was carried out under UV-B irradiation (centered at λ = 312 nm, 50 mW/cm^2, 30 min).

Denaturing Conditions and Recrystallization. DNA nanoparticle crystal samples were transferred to DNA denaturing conditions by addition of urea (7 M, 200 μL) followed by ultrasonication and heating above the DNA melting temperature (70 °C). DNA-functionalized NPs obtained from the de-cross-linking/DNA denaturation procedure were purified by centrifugation (16 400 rpm, 10 min), resuspended in 0.3 M NaCl, and annealed *via* a slow-cooling procedure as above to achieve recrystallization.

Preparation of Samples for Characterization. *TEM Imaging of Nanoparticles.* Nanoparticles' size and morphology were assessed by TEM. All samples were deposited as a droplet on carbon Film 400 mesh copper grids, and the solvent was evaporated.

SEM Imaging of Superlattices. To prevent the superlattice from collapsing under vacuum during SEM imaging, all the samples were encapsulated in a silica shell, following previously reported literature protocols.[48] After slow cooling, the samples were transferred to a 1.5 mL tube and reconstituted in a solution of NaCl (1 mL, 0.3 M). The tube was sonicated at room temperature, and *N*-trimethoxysilylpropyl-*N*,*N*,*N*-trimethylammonium chloride (2 μL) was added. After 20 min, 4 μL of a silica-growing agent, triethoxysilane, was added to the tube and allowed to stir for 4 days at room temperature. The mixture was purified by three rounds of centrifugation (700 rpm, 5 min) and redispersed in water. The sample for imaging was prepared by drop-casting 10 μL of the silica-embedded crystals onto a silicon wafer chip, which was left to dry.

Small Angle X-Ray Scattering Measurements. X-ray data was collected through in-situ small angle X-ray scattering (SAXS) at the 11-BM Complex Materials Scattering (CMS) beamline at the NSLSII facility at Brookhaven National Laboratory. Samples in buffer solution were loaded into glass capillary tubes and set onto a sample stage for scattering under ambient conditions and an exposure time of 10 s. The SAXS detector was a Pilatus 2M detector from Dectris, with measurement and beam conditions defined as detector distance = 5.02 m, wavelength = 0.918 Å, and energy = 13.5 KeV.

ASSOCIATED CONTENT

Supporting Information

The Supporting Information is available free of charge on the ACS Publications website at DOI: 10.1021/acsnano.9b01294.

Additional experimental detail and data including oligonucleotide synthesis, nanoparticle characterization, and superlattice characterization (PDF)

AUTHOR INFORMATION

Corresponding Authors

*E-mail: og2226@columbia.edu.

*E-mail: A.Kanaras@soton.ac.uk.

ORCID

Afaf H. El-Sagheer: 0000-0001-8706-1292

Iris Nandhakumar: 0000-0002-9668-9126

Matthew Richard Burton: 0000-0002-0376-6322

Tom Brown: 0000-0002-6538-3036

Otto L. Muskens: 0000-0003-0693-5504

Antonios G. Kanaras: 0000-0002-9847-6706

Notes

The authors declare no competing financial interest.

Raw data supporting this article can be found at https://eprints.soton.ac.uk/429701/.

ACKNOWLEDGMENTS

A.G.K. and A.F.D.F. would like to thank DSTL for funding of this project. The authors would also like to acknowledge the assistance provided by the Swansea University AIM Facility funded in part by EPSRC (EP/M028267/1), European Regional Development Fund via the Welsh Government (80708), and Sêr Solar. O.G. and J.K. were supported by the U.S. Department of Energy, Office of Basic Energy Sciences, Division of Materials Sciences and Engineering, under grant DE-SC0008772. A.H.E.S. was supported by UK BBSRC grant BB/J001694/2 (extending the boundaries of nucleic acid chemistry). M.R.B. was supported by EPSRC (EP/N020863/1). This research used resources of the Center for Functional Nanomaterials and the 11-BM Complex Materials Scattering (CMS) beamline, operated by the National Synchrotron Light Source II and the Center for Functional Nanomaterilas, which are U.S. Department of Energy (DOE) office of Science User Facilities operated for the DOE Office of Science by Brookhaven National Laboratory under Contract No. DE-SC0012704.

REFERENCES

(1) Nie, Z.; Petukhova, A.; Kumacheva, E. Properties and Emerging Applications of Self-Assembled Structures Made from Inorganic Nanoparticles. *Nat. Nanotechnol.* **2010**, *5*, 15−25.

(2) Grzelczak, M.; Vermant, J.; Furst, E. M.; Liz-Marzán, L. M. Directed Self-Assembly of Nanoparticles. *ACS Nano* **2010**, *4*, 3591−3605.

(3) Pileni, M. P.; Cozzoli, D. P.; Pinna, N. Self-Assembled Supracrystals and Hetero-Structures Made from Colloidal Nanocrystals. *CrystEngComm* **2014**, *16*, 9365−9367.

(4) Boles, M. A.; Engel, M.; Talapin, D. V. Self-Assembly of Colloidal Nanocrystals: From Intricate Structures to Functional Materials. *Chem. Rev.* **2016**, *116*, 11220−11289.

(5) Fery, A.; García de Abajo, F. J.; Liz-Marzán, L. M.; Wagner, C. S.; Wittemann, A.; Romo-Herrera, J. M.; Alvarez-Puebla, R. A.; Pazos-Perez, N. Organized Plasmonic Clusters with High Coordination Number and Extraordinary Enhancement in Surface-Enhanced Raman Scattering (SERS). *Angew. Chem., Int. Ed.* **2012**, *51*, 12688−12693.

(6) Tebbe, M.; Lentz, S.; Guerrini, L.; Fery, A.; Alvarez-Puebla, R. A.; Pazos-Perez, N. Fabrication and Optical Enhancing Properties of Discrete Supercrystals. *Nanoscale* **2016**, *8*, 12702−12709.

(7) Pileni, M. P. Self-Assembly of Inorganic Nanocrystals: Fabrication and Collective Intrinsic Properties. *Acc. Chem. Res.* **2007**, *40*, 685−693.

(8) Murray, C. B.; Kagan, C. R.; Bawendi, M. G. Self-Organization of CdSe Nanocrystallites into Three-Dimensional Quantum Dot Superlattices. *Science* **1995**, *270*, 1335−1338.

(9) Baranov, D.; Manna, L.; Kanaras, A. G. Chemically Induced Self-Assembly of Spherical and Anisotropic Inorganic Nanocrystals. *J. Mater. Chem.* **2011**, *21*, 16694−16703.

(10) Brust, M.; Schiffrin, D. J.; Bethell, D.; Kiely, C. J. Novel Gold-dithiol Nano-networks with Non-metallic Electronic Properties. *Adv. Mater.* **1995**, *7*, 795−797.

DOI: 10.1021/acsnano.9b01294
ACS Nano XXXX, XXX, XXX−XXX

(11) Whetten, R. L.; Khoury, J. T.; Alvarez, M. M.; Murthy, S.; Vezmar, I.; Wang, Z. L.; Stephens, P. W.; Cleveland, C. L.; Luedtke, W. D.; Landman, U. Nanocrystal Gold Molecules. *Adv. Mater.* **1996**, *8*, 428−433.
(12) Boal, A. K.; Ilhan, F.; DeRouchey, J. E.; Thurn-Albrecht, T.; Russell, T. P.; Rotello, V. M. Self-Assembly of Nanoparticles into Structured Spherical and Network Aggregates. *Nature* **2000**, *404*, 746−748.
(13) Lopes, W. A.; Jaeger, H. M. Hierarchical Self-Assembly of Metal Nanostructures on Diblock Copolymer Scaffolds. *Nature* **2001**, *414*, 735−738.
(14) Costanzo, P. J.; Beyer, F. L. Thermally Driven Assembly of Nanoparticles in Polymer Matrices. *Macromolecules* **2007**, *40*, 3996−4001.
(15) Fernandes, R.; Li, M.; Dujardin, E.; Mann, S.; Kanaras, A. G. Ligand-Mediated Self-Assembly of Polymer-Enveloped Gold Nanoparticle Chains and Networks. *Chem. Commun.* **2010**, *46*, 7602−7604.
(16) Giannini, V.; Alvarez-Puebla, R. A.; Pazos-Perez, N.; Fitzgerald, J. M.; Guerrini, L. Modular Assembly of Plasmonic Core−satellite Structures as Highly Brilliant SERS-Encoded Nanoparticles. *Nanoscale Adv.* **2019**, *1*, 122−131.
(17) Dickerson, M. B.; Sandhage, K. H.; Naik, R. R. Protein- and Peptide-Directed Syntheses of Inorganic Materials. *Chem. Rev.* **2008**, *108*, 4935−4978.
(18) Franzmann, E.; Khalil, F.; Weidmann, C.; Schröder, M.; Rohnke, M.; Janek, J.; Smarsly, B. M.; Maison, W. A Biomimetic Principle for the Chemical Modification of Metal Surfaces: Synthesis of Tripodal Catecholates as Analogues of Siderophores and Mussel Adhesion Proteins. *Chem. - Eur. J.* **2011**, *17*, 8596−8603.
(19) Song, C.; Wang, Y.; Rosi, N. L. Peptide-Directed Synthesis and Assembly of Hollow Spherical CoPt Nanoparticle Superstructures. *Angew. Chem., Int. Ed.* **2013**, *52*, 3993−3995.
(20) Coomber, D.; Bartczak, D.; Gerrard, S. R.; Tyas, S.; Kanaras, A. G.; Stulz, E. Programmed Assembly of Peptide-Functionalized Gold Nanoparticles on DNA Templates. *Langmuir* **2010**, *26*, 13760−13762.
(21) Kanaras, A. G.; Wang, Z.; Hussain, I.; Brust, M.; Cosstick, R.; Bates, A. D. Site-Specific Ligation of DNA-Modified Gold Nanoparticles Activated by the Restriction EnzymeStyI. *Small* **2007**, *3*, 67−70.
(22) Claridge, S. A.; Mastroianni, A. J.; Au, Y. B.; Liang, H. W.; Micheel, C. M.; Fréchet, J. M. J.; Alivisatos, A. P. Enzymatic Ligation Creates Discrete Multinanoparticle Building Blocks for Self-Assembly. *J. Am. Chem. Soc.* **2008**, *130*, 9598−9605.
(23) Mirkin, C. A.; Letsinger, R. L.; Mucic, R. C.; Storhoff, J. J. A DNA-Based Method for Rationally Assembling Nanoparticles into Macroscopic Materials. *Nature* **1996**, *382*, 607−609.
(24) Alivisatos, A. P.; Johnsson, K. P.; Peng, X.; Wilson, T. E.; Loweth, C. J.; Bruchez, M. P.; Schultz, P. G. Organization of ' Nanocrystal Molecules' Using DNA. *Nature* **1996**, *382*, 609−611.
(25) Park, S. Y.; Lytton-Jean, A. K. R.; Lee, B.; Weigand, S.; Schatz, G. C.; Mirkin, C. A. DNA-Programmable Nanoparticle Crystallization. *Nature* **2008**, *451*, 553−556.
(26) Nykypanchuk, D.; Maye, M. M.; van der Lelie, D.; Gang, O. DNA-Guided Crystallization of Colloidal Nanoparticles. *Nature* **2008**, *451*, 549−552.
(27) O'Brien, M. N.; Lin, H. X.; Girard, M.; Olvera De La Cruz, M.; Mirkin, C. A. Programming Colloidal Crystal Habit with Anisotropic Nanoparticle Building Blocks and DNA Bonds. *J. Am. Chem. Soc.* **2016**, *138*, 14562−14565.
(28) Zhang, C.; Macfarlane, R. J.; Young, K. L.; Choi, C. H. J.; Hao, L.; Auyeung, E.; Liu, G.; Zhou, X.; Mirkin, C. A. A General Approach to DNA-Programmable Atom Equivalents. *Nat. Mater.* **2013**, *12*, 741−746.
(29) Macfarlane, R. J.; O'Brien, M. N.; Petrosko, S. H.; Mirkin, C. a. Nucleic Acid-Modified Nanostructures as Programmable Atom Equivalents: Forging a New "Table of Elements. *Angew. Chem., Int. Ed.* **2013**, *52*, 5688−5698.
(30) Young, K. L.; Ross, M. B.; Blaber, M. G.; Rycenga, M.; Jones, M. R.; Zhang, C.; Senesi, A. J.; Lee, B.; Schatz, G. C.; Mirkin, C. A. Using DNA to Design Plasmonic Metamaterials with Tunable Optical Properties. *Adv. Mater.* **2014**, *26*, 653−659.
(31) Sun, D.; Gang, O. Binary Heterogeneous Superlattices Assembled from Quantum Dots and Gold Nanoparticles with DNA. *J. Am. Chem. Soc.* **2011**, *133*, 5252−5254.
(32) Lu, F.; Yager, K. G.; Zhang, Y.; Xin, H.; Gang, O. Superlattices Assembled through Shape-Induced Directional Binding. *Nat. Commun.* **2015**, *6* (1−10), 6912.
(33) Liu, W.; Tagawa, M.; Xin, H. L.; Wang, T.; Emamy, H.; Li, H.; Yager, K. G.; Starr, F. W.; Tkachenko, A. V.; Gang, O. Diamond Family of Nanoparticle Superlattices. *Science* **2016**, *351*, 582−586.
(34) Kim, Y.; Macfarlane, R. J.; Jones, M. R.; Mirkin, C. A. Transmutable Nanoparticles with Reconfigurable Surface Ligands. *Science* **2016**, *351*, 579−582.
(35) Seo, S. E.; Wang, M. X.; Shade, C. M.; Rouge, J. L.; Brown, K. A.; Mirkin, C. A. Modulating the Bond Strength of DNA−Nanoparticle Superlattices. *ACS Nano* **2016**, *10*, 1771−1779.
(36) Oh, T.; Park, S. S.; Mirkin, C. A. Stabilization of Colloidal Crystals Engineered with DNA. *Adv. Mater.* **2019**, *31* (1−5), 1805480.
(37) Kanaras, A. G.; Wang, Z.; Bates, A. D.; Cosstick, R.; Brust, M. Towards Multistep Nanostructure Synthesis: Programmed Enzymatic Self-Assembly of DNA/Gold Systems. *Angew. Chem., Int. Ed.* **2003**, *42*, 191−194.
(38) Heuer-Jungemann, A.; Kirkwood, R.; El-Sagheer, A. H.; Brown, T.; Kanaras, A. G. Copper-Free Click Chemistry as an Emerging Tool for the Programmed Ligation of DNA-Functionalised Gold Nanoparticles. *Nanoscale* **2013**, *5*, 7209−7212.
(39) Harimech, P. K.; Gerrard, S. R.; El-Sagheer, A. H.; Brown, T.; Kanaras, A. G. Reversible Ligation of Programmed DNA-Gold Nanoparticle Assemblies. *J. Am. Chem. Soc.* **2015**, *137*, 9242−9245.
(40) Yoshimura, Y.; Fujimoto, K. Ultrafast Reversible Photo-Cross-Linking Reaction: Toward *in Situ* DNA Manipulation. *Org. Lett.* **2008**, *10*, 3227−3230.
(41) Sakamoto, T.; Tanaka, Y.; Fujimoto, K. DNA Photo-Cross-Linking Using 3-Cyanovinylcarbazole Modified Oligonucleotide with Threoninol Linker. *Org. Lett.* **2015**, *17*, 936−939.
(42) Auyeung, E.; Li, T. I. N. G.; Senesi, A. J.; Schmucker, A. L.; Pals, B. C.; de la Cruz, M. O.; Mirkin, C. A. DNA-Mediated Nanoparticle Crystallization into Wulff Polyhedra. *Nature* **2014**, *505*, 73−77.
(43) Hurst, S. J.; Lytton-Jean, A. K. R.; Mirkin, C. A. Maximizing DNA Loading on a Range of Gold Nanoparticle Sizes. *Anal. Chem.* **2006**, *78*, 8313−8318.
(44) Warren, B. E. *X-Ray Diffraction*, New ed.; Dover Publications: New York, NY, 1990.
(45) Bastús, N. G.; Merkoçi, F.; Piella, J.; Puntes, V. Synthesis of Highly Monodisperse Citrate-Stabilized Silver Nanoparticles of up to 200 Nm: Kinetic Control and Catalytic Properties. *Chem. Mater.* **2014**, *26*, 2836−2846.
(46) Turkevich, J.; Stevenson, P. C.; Hillier, J. A Study of the Nucleation and Growth Processes in the Synthesis of Colloidal Gold. *Discuss. Faraday Soc.* **1951**, *55*, 55−75.
(47) Schulz, F.; Homolka, T.; Bastús, N. G.; Puntes, V.; Weller, H.; Vossmeyer, T. Little Adjustments Significantly Improve the Turkevich Synthesis of Gold Nanoparticles. *Langmuir* **2014**, *30*, 10779−10784.
(48) Auyeung, E.; Macfarlane, R. J.; Choi, C. H. J.; Cutler, J. I.; Mirkin, C. A. Transitioning DNA-Engineered Nanoparticle Superlattices from Solution to the Solid State. *Adv. Mater.* **2012**, *24*, 5181−5186.

DOI: 10.1021/acsnano.9b01294
ACS Nano XXXX, XXX, XXX−XXX